Supplementary information

Persistent and polarized global actin flow controls directionality during cell migration

Contents

I. Basic fluid-mechanics model for a cell 2

II. Extended fluid-mechanics model for a cell 7

References 10

In this document we derive the equations of the basic and extended cell fluid-mechanical models used in the main text to describe the striking experimental observations, including symmetry breaking and the emergence of stable flows, actin sink and myosin II accumulation at the rear of cell front, high persistence of cell migration, sensitivity of flows to changes in myosin II, and robustness of flows to changes in cofilin.

I. BASIC FLUID-MECHANICS MODEL FOR A CELL

The basic model is very similar to the 1D flow models in [1] used to explain spontaneous symmetry breaking and emergence of flows (see also [2, 3]). This model contains three molecular species, cortical actin (F-actin) with density ρ, cytosolic myosin II with concentration c, and cortical myosin II with density μ. These line densities depend on angle $\theta = [-\pi, \pi]$ and time t. The spatial-temporal dynamics are given by

$$\partial_t \rho + R^{-2}\partial_\theta(\rho \partial_\theta \Psi) = k_p - k_d \rho \tag{S1}$$

$$\partial_\theta(-\zeta\mu - \alpha\rho + \beta R^{-2}\partial_\theta^2 \rho) = \xi \partial_\theta \Psi \tag{S2}$$

$$\partial_t c = D_c R^{-2}\partial_\theta^2 c - k^{\mathrm{on}} c + k^{\mathrm{off}} \mu \tag{S3}$$

$$\partial_t \mu + R^{-2}\partial_\theta(\mu \partial_\theta \Psi) = k^{\mathrm{on}} c - k^{\mathrm{off}} \mu + D_\mu R^{-2}\partial_\theta^2 \mu, \tag{S4}$$

where Eq. S1 describes actin polymerisation (with k_p) and depolymerisation (with k_d), Eq. S2 describes the irrotational cortical flow with velocity $v = (1/R)\partial_\theta \Psi$ due to active stress from contraction by myosin ($-\zeta\mu$) and an actin-induced pressure ($P = \alpha\rho - \beta R^{-2}\partial_\theta^2 \rho$).

Parameter ξ denotes the friction with the external environment, α^{-1} is the compressibility of the gel, and $\sqrt{\beta/\alpha}$ is the correlation length of the density fluctuations. Generally, we neglect internal viscous effects of the gel. Eqs. S3 and S4 describe the cytosolic and cortical myosin, including binding (with k^{on}) and unbinding (with k^{off}) to the cortex, as well as diffusion (with D_c in cytosol and with D_μ in cortex).

The homogeneous steady state values are derived as follows. From Eq. S1 we obtain

$$\rho_0 = \frac{k_p}{k_d}, \tag{S5}$$

and from Eq. S3 we obtain

$$c_0 = \frac{k^{\text{off}}\mu_0}{k^{\text{on}}} \tag{S6}$$

with parameter μ_0 being freely adjustable.

To understand when the homogeneous steady state becomes unstable in this active system, we conduct linear stability analysis, where we expand around the steady state to linear order using fluctuations

$$\rho(\theta,t) = \rho_0 + \delta\rho(\theta,t) \tag{S7}$$

$$c(\theta,t) = c_0 + \delta c(\theta,t) \tag{S8}$$

$$\mu(\theta,t) = \mu_0 + \delta\mu(\theta,t). \tag{S9}$$

This allows us to obtain for the linearised dynamics

$$\partial_t(\delta\rho) = \left[-\frac{\rho_0}{\xi R^2}\left(\frac{\beta}{R^2}\partial_\theta^4 - \alpha\partial_\theta^2\right) - k_d\right]\delta\rho + \frac{\rho_0\zeta}{\xi R^2}\partial_\theta^2\delta\mu \tag{S10}$$

$$\partial_t(\delta\mu) = -\frac{\mu_0}{\xi R^2}\left(\frac{\beta}{R^2}\partial_\theta^4 - \alpha\partial_\theta^2\right)\delta\rho + \left[\frac{\mu_0\zeta}{\xi R^2}\partial_\theta^2 - k^{\text{off}} + \frac{D_\mu}{R^2}\partial_\theta^2\right]\delta\mu + k^{\text{on}}\delta c \tag{S11}$$

$$\partial_t(\delta c) = k^{\text{off}}\delta\mu + \left(\frac{D_c}{R^2}\partial_\theta^2 - k^{\text{on}}\right)\delta c. \tag{S12}$$

Next, we Fourier transform via substitutions $\partial_\theta^4 \to i^4k^4 = k^4$ and $\partial_\theta^2 \to i^2k^2 = -k^2$ in order to remove the spatial derivatives at the expense of introducing a new variable, the wave number k. To obtain the dispersion relation $s(k)$, i.e. how the eigenvalue s depends on wave

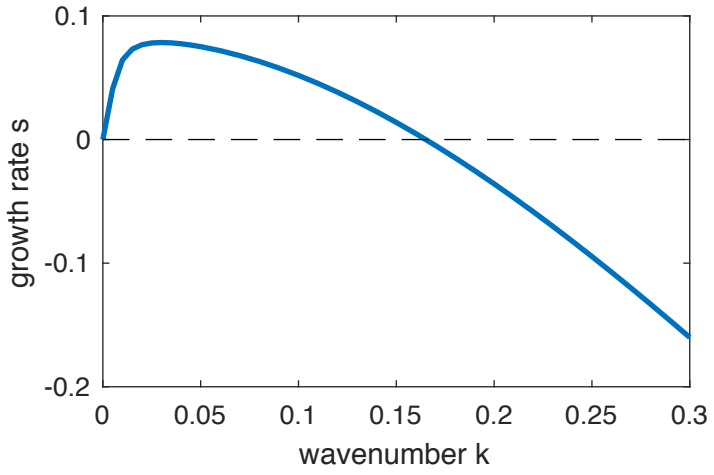

FIG. S1: Growth rate of deviations from the homogeneous steady state as a function of the spatial wavenumber, k. Positive growth rates indicate pattern formation, and the first non-zero spatial mode, $l = 1$, is located at $k = l/R = 0.1$.

number k, we need to solve the characteristic polynomial, given by the expression

$$\begin{aligned}&\left[-\frac{\rho_0}{\xi R^2}\left(\frac{\beta}{R^2}k^4+\alpha k^2\right)-k_d-s\right]\\&\quad\cdot\left[\left(\frac{\mu_0\zeta}{\xi R^2}k^2+k^{\text{off}}+\frac{D_\mu}{R^2}k^2+s\right)\left(\frac{D_c}{R^2}k^2+k^{\text{on}}+s\right)-k^{\text{on}}k^{\text{off}}\right]\\&+\frac{\rho_0\zeta}{\xi R^2}k^2\cdot\frac{\mu_0}{\xi R^2}\left(\frac{\beta}{R^2}k^4+\alpha k^2\right)\left(\frac{D_c}{R^2}k^2+k^{\text{on}}+s\right)=0.\end{aligned}\tag{S13}$$

The wave number can be expressed as $k = l/R$ with $l = 0, 1, 2, ...$, where $l = 1$ is the first non-homogeneous mode we are interested in. In particular, we are interested in understanding when the real part of $s(l = 1)$ becomes positive and hence the homogeneous steady state unstable. A key parameter to characterise the activity in this system is the unitless Péclet number, which describes the ratio of advective and diffusive tendencies and is given by Pé$= -\zeta\mu_0/(\tilde{D}\xi)$ with the effective time-averaged diffusion constant $\tilde{D} = (D_c k^{\text{off}} + D_\mu k^{\text{on}})/k^{\text{on}}$. For a sufficiently high Pé number, the real part is indeed positive, plotted in Fig. S1.

We can further characterise the emergence of foci, i.e., pattern formation, as a function of the model parameters. Considering the first non-zero spatial mode, $l = 1$, we see that the growth rate of fluctuations requires threshold values of both actin depolymerisation rate, k_d, and homogeneous steady state myosin concentration, μ_0 (Fig. S2). We further note that

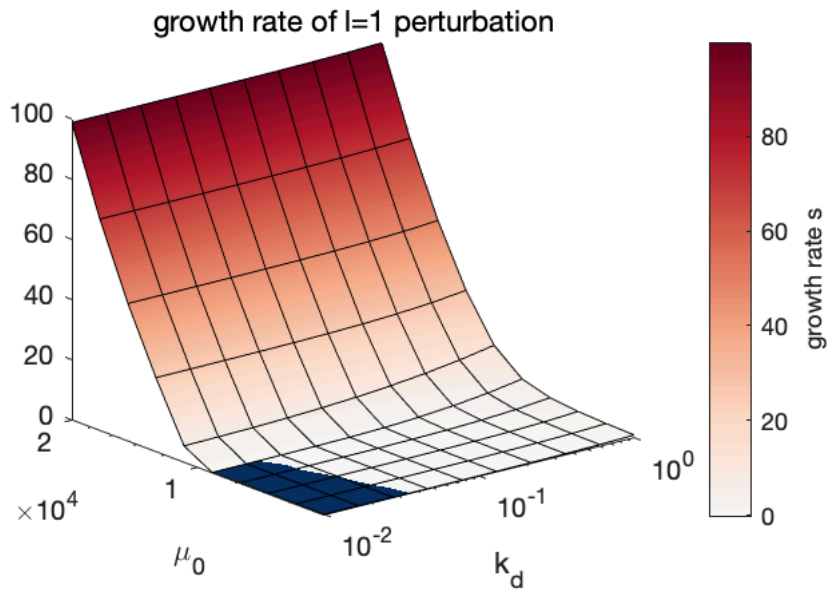

FIG. S2: Growth rate of fluctuations from the homogeneous steady state with spatial mode $l = 1$ as a function of actin depolymerisation rate, k_d, and homogeneous steady state myosin concentration, μ_0. Positive growth rates indicate pattern formation, and negative growth rates (here clipped at zero for visual emphasis) return to the homogeneous steady state.

the pattern formation rate is much less sensitive to the actin depolymerisation rate, which might reflect the observed robustness of the flow pattern to changes in cofilin levels, than it is to myosin levels, which might reflect the observed sensitivity to myosin II levels (see main text).

We solve the model numerically as a system of differential algebraic equations, with $v = (1/R)\partial_\theta \Psi$ as the algebraic variable. We use Mathematica's NDSolve, with periodic boundary conditions and a MaxStepFraction of 1/100. For initial conditions we add a small fluctuation to the homogeneous steady state in the form of $\kappa \cos(\theta - \pi)$ with $\kappa = 0.01$. We observed that a steady state was reached by $T = 150$s, and that the resulting pattern did not change appreciably for longer solution times (though this will depend on the parameters used).

To investigate the robustness to perturbations, we apply a perturbation of the form

$$\rho_p = s\left[e^{-(\theta-\theta_p)^2} + e^{-(\theta-(\theta_p+2\pi))^2} + e^{-(\theta-(\theta_p-2\pi))^2}\right] \tag{S14}$$

$$\partial_\theta \Psi_p = \partial_\theta(-\alpha\rho_p + \beta R^{-2}\partial_\theta^2\rho_p)/\xi \tag{S15}$$

on top of the steady state flows, where the functional form of the perturbation is chosen to satisfy the periodic boundary condition, θ_p is the angular location of the perturbation, and s is the strength of the perturbation relative to the height of actin peak at steady state. The perturbation in actin is added to the steady state, and the corresponding instantaneous change in the flow, $\partial_\theta\Psi_p$, is calculated to satisfy the system of differential-algebraic equations (treating $\partial_\theta\Psi_p/R = v$ as the variable to solve for numerically). To investigate how the steady state is altered by this perturbation, the system is solved numerically with initial conditions $\rho = \rho^* + \rho_p, v = v^* + v_p, \mu = \mu^*, c = c^*$, where * denotes the steady-state value of the variable before the perturbation is applied. A new steady state was typically reached after a few to tens of seconds of solution time.

This result shows that flows are exceptionally stable, which directly translate to highly persistent cell motion. To see this, cell speed results from force balancing the retrograde actin flow due to friction with the viscous external fluid, leading to a propulsive force on the cell. To linear order this is given by $F_p = (8\pi/3)h_0R^2\xi v_0$, where h_0 is the cortical thickness and v_0 is the amplitude of the cortical flows [1]. Hence, if the intracellular flow is stable, then cell motion is also stable and persistent.

Parameters are given in Table I, with $\zeta = -\mathrm{Pe}\cdot\xi\cdot(D_c k^{\mathrm{off}} + D_\mu k^{\mathrm{on}})/(k^{\mathrm{on}}\mu_0)$.

TABLE I: **Parameters used for basic model**

	Description	Value	Units
ξ	friction with substrate	0.1	kg/(μm^3 s)
k^{on}	myosin binding rate	1	s^{-1}
k^{off}	myosin unbinding rate	0.1	s^{-1}
D_μ	cortical myosin diffusivity	1	μm^2/s
D_c	cytosol myosin diffusivity	10	μm^2/s
β	correlation length $\sqrt{\beta/\alpha}$	10^3	kg/(μm s^2)
α	inverse compressibility	10^3	kg/(μm s^2)
k_d	actin depolymerisation rate	0.1	s^{-1}
R	cell radius	10	μm
μ_0	steady-state myosin concentration	10^4	μm^{-1}
Pe	Péclet number	2500	–

II. EXTENDED FLUID-MECHANICS MODEL FOR A CELL

Here, we extend the basic model to more realistic dynamics for actin and myosin. In particular, we assume that in Eq. S1 actin polymerisation is self-activating (with saturation) [4] and that the myosin II-induced stress promotes depolymerisation as contraction should make F actin brittle [5]. We further assume that in Eqs. S3 and S4 myosin II binding to the cortex is F actin dependent as F actin is the substrate for myosin II. As a result we obtain the modified equations

$$\partial_t \rho + R^{-2}\partial_\theta(\rho\partial_\theta\Psi) = k_p\frac{\rho^2}{K^2+\rho^2} - k_d\mu\rho \tag{S16}$$

$$\partial_\theta(-\zeta\mu - \alpha\rho + \beta R^{-2}\partial_\theta^2\rho) = \xi\partial_\theta\Psi \tag{S17}$$

$$\partial_t c = D_c R^{-2}\partial_\theta^2 c - k^{\mathrm{on}}\rho c + k^{\mathrm{off}}\mu \tag{S18}$$

$$\partial_t \mu + R^{-2}\partial_\theta(\mu\partial_\theta\Psi) = k^{\mathrm{on}}\rho c - k^{\mathrm{off}}\mu + D_\mu R^{-2}\partial_\theta^2\mu \tag{S19}$$

which we again solve numerically with Mathematica as a system of differential algebraic equations, with $v = (1/R)\partial_\theta\Psi$ as the algebraic variable.

The homogeneous steady state is again obtained as follows. From Eq. S16 we obtain

condition

$$k_p \frac{\rho^2}{K^2+\rho^2} = k_d \mu_0 \rho_0 \tag{S20}$$

and hence

$$\rho_{1,2} = \frac{k_p}{2k_d\mu_0} \pm \sqrt{\frac{k_p^2}{(2k_d\mu_0)^2} - K^2} \tag{S21}$$

with monostability for $K = K_c = k_p/(2k_d\mu_0)$. If bistable, the upper state is stable. From Eq. S18 we obatin condition

$$k^{\mathrm{on}} \rho_0 c_0 = k^{\mathrm{off}} \mu_0 \tag{S22}$$

and hence $c_0 = k^{\mathrm{off}}\mu_0/(k^{\mathrm{on}}\rho_0)$. Parameter μ_0 is freely adjustable.

To conduct the linear stability analysis, we expand around the steady state to linear order using again Eqs. S7-S9, and obtain for the linearised dynamics

$$\begin{aligned}
\partial_t(\delta\rho) &= \left[-\frac{\rho_0}{\xi R^2}\left(\frac{\beta}{R^2}\partial_\theta^4 - \alpha\partial_\theta^2\right) + k_p \frac{2K^2\rho_0}{(K^2+\rho_0^2)^2} - k_d\mu_0\right]\delta\rho \\
&\quad + \left[\frac{\rho_0\zeta}{\xi R^2}\partial_\theta^2 - k_d\rho_0\right]\delta\mu \qquad \text{(S23)} \\
\partial_t(\delta\mu) &= \left[-\frac{\mu_0}{\xi R^2}\left(\frac{\beta}{R^2}\partial_\theta^4 - \alpha\partial_\theta^2\right) + k^{\mathrm{on}}c_0\right]\delta\rho + \left[\frac{\mu_0\zeta}{\xi R^2}\partial_\theta^2 - k^{\mathrm{off}} + \frac{D_\mu}{R^2}\partial_\theta^2\right]\delta\mu \\
&\quad + k^{\mathrm{on}}\rho_0\delta c \qquad \text{(S24)} \\
\partial_t(\delta c) &= -k^{\mathrm{on}}\delta\rho + k^{\mathrm{off}}\delta\mu + \left[\frac{D_c}{R^2}\partial_\theta^2 - k^{\mathrm{on}}\rho_0\right]\delta c, \qquad \text{(S25)}
\end{aligned}$$

which we again Fourier transform. To obtain the dispersion relation $s(k)$, we solve the characteristic polynomial, given by the lengthy expression

$$\begin{aligned}
&\left[-\frac{\rho_0}{\xi R^2}\left(\frac{\beta}{R^2}k^4 + \alpha k^2\right) + k_p\frac{2K^2\rho_0}{(K^2+\rho_0^2)^2} - k_d\mu_0 - s\right] \\
&\quad\cdot\left[\left(\frac{\mu_0\zeta}{\xi R^2}k^2 + k^{\mathrm{off}} + \frac{D_\mu}{R^2}k^2 + s\right)\left(\frac{D_c}{R^2}k^2 + k^{\mathrm{on}}\rho_0 + s\right) - k^{\mathrm{on}}k^{\mathrm{off}}\rho_0\right] \\
&+\left(\frac{\rho_0\zeta}{\xi R^2}k^2 + k_d\rho_0\right) \\
&\quad\cdot\left[\left(\frac{\mu_0}{\xi R^2}\left(\frac{\beta}{R^2}k^4 + \alpha k^2\right) - k^{\mathrm{on}}c_0\right)\left(\frac{D_c}{R^2}k^2 + k^{\mathrm{on}}\rho_0 + s\right) + \left(k^{\mathrm{on}}\right)^2 c_0\rho_0\right] = 0 \qquad \text{(S26)}
\end{aligned}$$

The wave number can again be expressed as $k = l/R$ with $l = 0, 1, 2, ...$, where $l = 1$ is the first non-homogeneous mode we are interested in. When is the real part of $s(l = 1)$ positive and hence the homogeneous steady state unstable? For this purpose, we again consider the unitless Péclet number, now given by Pé$= -\zeta\mu_0/(\tilde{D}\xi)$ with the effective time-averaged diffusion constant $\tilde{D} = (D_c k^{\mathrm{off}} + D_\mu\rho_0 k^{\mathrm{on}})/(\rho_0 k^{\mathrm{on}})$. For a sufficiently high Pé number, the

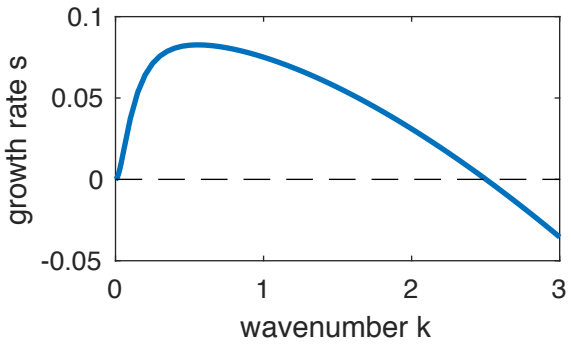

FIG. S3: Growth rate of deviations from the homogeneous steady state as a function of the spatial wavenumber, k. Positive growth rates indicate pattern formation, and the first non-zero spatial mode, $l = 1$, is located at $k = l/R = 0.1$.

real part is indeed positive, plotted in Fig. S3.

We solve the model numerically as a system of differential algebraic equations, as for the basic model, but now for $T = 300s$ and with a MaxStepFraction of 1/200. We further reduced the AccuracyGoal and PrecisionGoal to allow Mathematica's solver to compute the pattern formation instability at the given discretization without error (the solution errors can otherwise appear to be large as the initial condition is, by design, unstable).

To investigate the robustness to perturbations, we again apply a perturbation in ρ (S14), add this to the steady state values of the variables ρ, v, μ, c, to obtain a new initial condition from which we solve numerically until a new steady state is reached.

Parameters are given in Table II, with $\zeta = -\mathrm{Pe} \cdot \xi \cdot (D_c k^{\mathrm{off}} + D_\mu k^{\mathrm{on}} \rho_0)/(k^{\mathrm{on}} \rho_0 \mu_0)$. Note that with respect to the basic model k^{on} was replaced by $k^{\mathrm{on}}\rho_0$, where $\rho_0 = k_p/(2k_d\mu_0) + \sqrt{k_p^2/(2k_d\mu_0)^2 - K^2}$.

TABLE II: **Parameters used for extended model**

	Description	Value	Units
ξ	friction with substrate	0.1	kg/(μm^3 s)
k_{on}	myosin binding rate	10^{-4}	μm/s
k_{off}	myosin unbinding rate	0.1	s^{-1}
D_μ	cortical myosin diffusivity	1	μm^2/s
D_c	cytosol myosin diffusivity	10	μm^2/s
β	correlation length $\sqrt{\beta/\alpha}$	10^{-2}	kg/(μm s^2)
α	inverse compressibility	10^{-2}	kg/(μm s^2)
k_d	actin depolymerisation rate	10^{-5}	μm/s
k_p	actin polymerisation rate	10^3	(μm s)$^{-1}$
R	cell radius	10	μm
μ_0	steady-state myosin concentration	10^4	μm^{-1}
Pe	Péclet number	5	–
K	Actin polymerisation theshold	$0.2K_c = \frac{0.1k_p}{k_d\mu_0}$	μm^{-1}

[1] Hawkins RJ, Poincloux R, Bnichou O, Piel M, Chavrier P, Voituriez R. Biphys J 101: 1041 (2011)

[2] Jülicher F, Kruse K, Prost J, Joanny J-F. Phys Rep 449: 3 (2007)

[3] Bois JS, Jülicher F, Grill SW. Phys Rev Lett 106: 028103 (2011)

[4] Weiner OD, Marganski WA, Wu LF, Altschuler SJ, Kirschner MW. PLoS Biol 5: e221 (2007)

[5] Bretschneider T, Anderson K, Ecke M, Mller-Taubenberger A, Schroth-Diez B, Ishikawa-Ankerhold HC, Gerisch G. Biophys J 96: 2888 (2009)